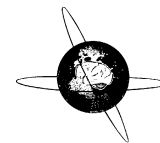




Contents lists available at ScienceDirect

Clinical Neurophysiology

journal homepage: www.elsevier.com/locate/clinph

Impaired mesial synchronization in temporal lobe epilepsy

Guillermo J. Ortega^{a,*}, Iván Herrera Peco^{a,c}, Rafael G. Sola^{a,c}, Jesús Pastor^{b,c}

^a Department of Neurosurgery, Hospital Universitario de La Princesa, Madrid, Spain

^b Department of Clinical Neurophysiology, Hospital Universitario de La Princesa, Madrid, Spain

^c School of Medicine, San Pablo-CEU University, Madrid, Spain

ARTICLE INFO

Article history:

Accepted 4 November 2010

Available online xxx

Keywords:

Temporal lobe epilepsy

Synchronization

Clusters

Foramen ovale electrodes

Video-electroencephalography

Complexity

ABSTRACT

Objective: Temporal lobe epilepsy is commonly associated with synchronous, hyper-synchronous and des-synchronous activity. The aim of the present work is to explore synchronization activity in both mesial areas in temporal lobe epileptic patients during the interictal state.

Methods: Using a cluster technique, we analyzed 17 temporal lobe epilepsy patients' records of foramen ovale electrodes activity during the inter-ictal state.

Results: There exists a clear tendency in the mesial area of the epileptic side to be organized as isolated clusters of electrical activity as compared with the contra-lateral side, which is organized in the form of large clusters of synchronous activity. The number of desynchronized areas is larger in the epileptic side than in the contra-lateral side in 16 out of 17 temporal lobe epileptic patients.

Conclusions: The mesial area responsible for the seizures is less synchronous than the contra-lateral; the different kind of synchronous organization accounts for a lower synchronization activity at the epileptic side, suggesting that this lack of synchronous cluster organization would favour the appearance of seizures.

Significance: Our results shed new light regarding synchronization issues in temporal lobe epilepsy and also it would help in reducing drastically the time of study.

© 2010 International Federation of Clinical Neurophysiology. Published by Elsevier Ireland Ltd. All rights reserved.

1. Introduction

Synchronization, hyper-synchronization and de-synchronization are tightly associated with epilepsy (Netoff and Schiff, 2002; Mormann et al., 2003; Gutkin et al., 2001; Traub and Wong, 1982; Penfield and Jasper, 1954; Schindler et al., 2007). The classical view (Dichter and Ayala, 1987; Kandel et al., 2000) postulates that epileptic activity, appearing as interictal epileptiform discharges (IED) is caused by the hyper-synchronously depolarization shift followed by an after-hyperpolarization in thousand of neurons typically located in the hippocampal and parahippocampal region. While this behavior remains confined at this location, there may be no clinical manifestation, even though synchronous activity can be detected as IED or sharp waves in the electroencephalogram (EEG). As seizure starts, the magnitude of the after-hyperpolarization decreases and neurons generate continuous firing of action potentials. The inhibition surrounding the seizure “focus” weakens and the seizure then spread from the seizure onset zone, activating synchronously large populations of neurons at distant areas (Kandel et al., 2000), corre-

sponding to clinical manifestations of epileptic seizures, commonly characterized as “hypersynchronous states”. Several works (Netoff and Schiff, 2002; Mormann et al., 2003; Gutkin et al., 2001; Schindler et al., 2007) however, has apparently challenged this traditional view demonstrating that desynchronous activity is essential for the initiation and maintenance of epileptic seizures. Far from contradicting the classical knowledge, recent desynchronization results shed new light in the fragmented understanding we have today of the complex process which sparks and sustain a developed and extended hypersynchronization activity during the clinical seizure. It is now fairly evident that in temporal lobe epilepsy (TLE) the whole epileptogenic process is associated with dramatic changes in neuronal synchronization at several, both temporal and spatial, scales mainly in the mesial region, amygdala, hippocampus and entorhinal cortex, the major structures affected in this pathology.

The aim of the present work is to study how is organized the synchronous activity in the mesial area of the temporal lobe in patients suffering from TLE through the analysis of foramen ovale electrodes (FOE) (Wieser et al., 1985), during the inter-ictal state. Most of the past publications regarding interictal FOE analysis rest almost exclusively on traditional IED analysis (Engel, 1989; Pastor et al., 2006) to characterize/lateralize/localize epileptogenic areas. Little attention (see, however, Weber et al., 1998) has been given to nonlinear and synchronization analysis regarding FOE activity.

* Corresponding author. Address: Hospital Universitario de la Princesa, Departamento de Neurocirugía (planta 7), Diego de León 62, Madrid 28006, Spain. Tel.: +34 915202200x3637; fax: +34 915202560.

E-mail address: gjortega.hlpr@salud.madrid.org (G.J. Ortega).

This fact differs from the case of mesial activity recorded by using Intra-Hippocampal Depth Electrodes (IHDE) (Mormann et al., 2000; Andrzejak et al., 2006; Bartolomei et al., 2008; Bettus et al., 2008). In those cases, higher levels (local, global and/or band limited) of hippocampal synchronization during the interictal activity in the epileptic side were reported. Somewhat surprisingly, by analyzing FOE records instead of IHDE, we have found apparently dissimilar results to those previously published (Mormann et al., 2000; Andrzejak et al., 2006; Bettus et al., 2008). Through a broad band analysis, we will show here the existence of an imbalance regarding the synchronous organization between the epileptic and the contra-lateral side in TLE patients. Our results show higher levels of synchronous activity in the contra-lateral side as compared with the ipsi-lateral side. We have characterized synchronization in term of synchronization clusters. To perform this task, we have used a classical cluster technique.

2. Methods

2.1. Patients

A total of 17 patients (eight men and nine women) were included in this study (Table 1). The mean age and time of these intractable epilepsies were 35 ± 6.28 and 26.5 ± 10.7 years, respectively. This research was approved by the Ethical Committee of the Hospital de la Princesa. Informed consent was obtained from all patients. Patients were evaluated pre-surgically according to La Princesa's protocol, as published elsewhere (Pastor et al., 2005; Sola et al., 2005). Briefly, all patients were studied with interictal single photon emission computer tomography (SPECT), magnetic resonance imaging (MRI) 1.5 T, scalp EEG and video-electroencephalography (v-EEG) using 19 scalp electrodes according to the international 10–20 system. In Table 1 we show the clinical information and results of the pre-surgical studies routinely performed in the sample of TLE patients, as SPECT, MRI and v-EEG analysis. During the v-EEG recording, antiepileptic drugs were progressively removed from the second day to the fourth day (approximately one third dose per day). All patients had tried several anti-epileptic drugs (AED) in different combinations. At moment of v-EEG recording 1 patient had one AED, 7 patients had 2 and 9 patients had 3 drugs. We also include the overall physician diagnosis regarding lateralization. When surgery was performed, the kind of surgery

and outcome, in terms of Engel scale (Engel et al., 1993), is also included.

Six-contact platinum FOE with 1-cm center-to-center spacing (AD-Tech, Racine, USA) were inserted bilaterally under general anesthesia (Wieser and Schwarz, 2001; Pastor et al., 2008). The correct implantation was always assured by using fluoroscopic imaging in the operating room (Fig. 1A). We named FOE#1 to the most rostral electrode in the foramen ovale (see Fig. 1B), and FOE#6 to the most occipital one.

2.2. Signal analysis

Digital EEG and FOE data, acquired at 500 Hz, filtered at 0.5–60 Hz for both scalp and FOE recording, and exported at 200 Hz to ASCII format (XLTEK, Canada) were used. Artifact free epochs lasting around 60 min were selected for future numerical analysis, yielding an overall time of about 30 h. In all cases, multivariate temporal non-overlapping windows of 2048 data points were used. All derivations, scalp and FOE electrodes were referenced to $(Fz + Cz + Pz)/3$. Main results were verified by using as a common reference the average of all the scalp electrodes. We avoid bipolar montages because it would be impossible to describe unambiguously any spatial synchronization pattern. However, IED analysis was made by the expert neurophysiologist with bipolar montages.

Fig. 1C shows a typical record of FOE. Data were post-processed using Fortran and R programs.

In each temporal window of 2048 points, cross-correlation was calculated among the 28 electrodes' time series, 16 EEG electrodes and 12 FOE. When used in neurophysiological data, cross correlation performs in a similar fashion as phase correlations methods, e.g., coherence and phase synchronization (Quiñ Quiroga et al., 2002; Ortega et al., 2008; Netoff and Schiff, 2002), but avoiding the "dangerous phase" problem in these kinds of methods (Fein et al., 1988; Guevara et al., 2005). The Pearson correlation coefficient δ_{ij} at zero lag between two time series was calculated:

$$\delta_{ij}(0) = \frac{\sum_{k=1}^{N_{win}} (x_i(k) - \bar{x}_i)(x_j(k) - \bar{x}_j)}{\sqrt{\sum_{k=1}^{N_{win}} (x_i(k) - \bar{x}_i)^2 \sum_{k=1}^{N_{win}} (x_j(k) - \bar{x}_j)^2}} \quad (1)$$

where $\mathbf{x} = x_i(k)$, $i = 1, N_{chan}$ and $k = 1, N_{win}$ is each of the 28 (N_{chan}) channels of 2048 (N_{win}) data points.

Table 1

Clinical data of patients included in this study. Outcome column correspond to the Engel classification scheme (Engel et al., 1993).

Patients/seizure						Pre-surgical studies			Diagnosis and surgery		
Patient	Sex	Age (years)	History (years)	Type of seizure	Freq.	SPECT	MRI	v-EEG (inter/ictal)	Diag	Cx	Out come
1	Fe	31	29	PC	w	L M	Normal	LM/LM	L	L AMTR	I
2	Fe	36	35	PC	w	R M	R MS	RM/RM	R	R AMTR	I
3	Fe	37	6	PC	d	L M	Normal	RM/RM	R	R AMTR	I
4	Ma	48	43	SG	m	L M	R MS	RTM/RM	R	R AMTR	I
5	Ma	25	9	PC	d	R M	R MS	RM (FrBi)/RM	R	R AMTR	I
6	Ma	30	21	PC	w	LT	L cyst	Bi/LM	L	L AMTR	I
7	Ma	41	40	SG	irreg	LT	L MS	LM/LM	L	No	–
8	Fe	28	27	PSC	w	aLM	L MS	LM/LM	L	No	–
9	Fe	27	19	PSC	w	aLM	L MS	LM/LM	L	L AMTR	I
10	Ma	43	40	PC	m	aLM	L MS	Bi/LM	L	L AMTR	I
11	Ma	32	31	PC	w	aLM	L MS	LM/LM	L	L AMTR	I
12	Fe	37	28	SG	d	TM Bi (L > R)	R MS	Mult/RM	R	R AMTR	III
13	Ma	35	17	PC	w	extenTPI	L atrophy	Mult/LM	L	L AMTR	I
14	Fe	42	28	PC	w	aLM	M asim	Bi M/LM	L	L AMTR	I
15	Fe	34	33	SG	m	aMBi (L>>R)	R MS	RM/RM	R	No	–
16	Ma	30	15	PC	w	aLM	L MS	LM/LM	L	No	–
17	Fe	39	30	PC	w	LT	L Hipp S	Bi M/LM	L	No	–

Diag: Diagnosis; Freq: Seizure Frequency; Cx: Surgery; PC: Partial Complex; SG: Second. General; w: weekly; d: daily; m: monthly; irreg: irregular; L: Left.

R: Right; M: Mesial; T: temporal; P: Parietal; a: anteromedial; Bi: Bilateral; exten: extended; S: Sclerosis; Fr: Frontal; Mult: Multifocal; asim: asymmetry.

Ma: Male; Fe: Female; AMTR: Antero-Mesial Temporal Lobectomy.

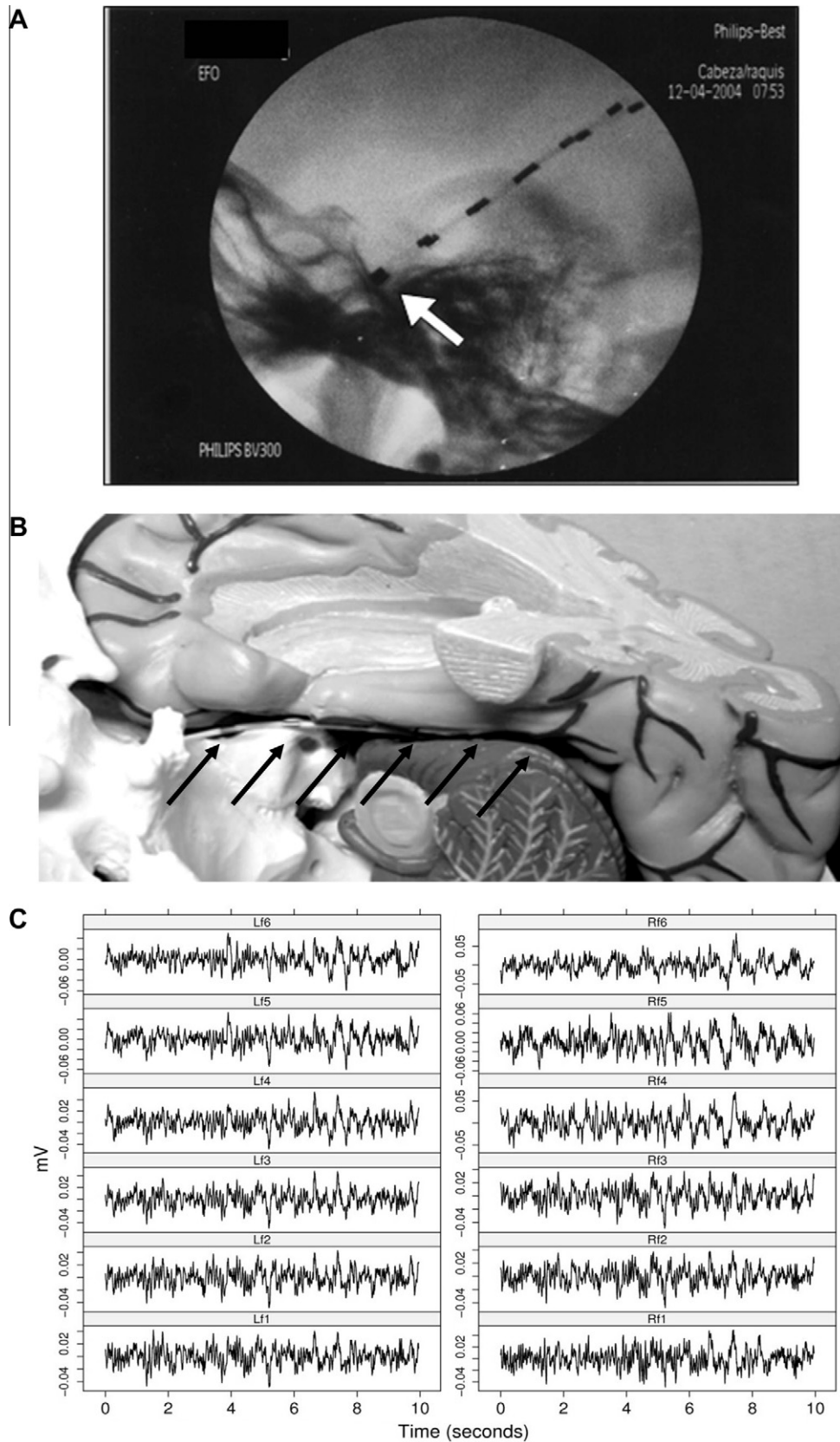


Fig. 1. Foramen ovale electrodes (A) Lateral view of the fluoroscopy performed in the operating room showing the final placement of the electrodes. FOE#1 is placed at the inner side of the foramen ovale (arrow). (B) Mesial aspect of the right temporal lobe and the right cerebellar hemisphere in a model of brain and skull. A foramen ovale electrode (FOE) was introduced through the right foramen ovale in order to demonstrate its localization within the mesial structures. Note that FOE and the temporal lobe are not in parallel (Wieser and Schwarz, 2001). Arrows indicate FOE locations. (C) Representative segments of FOE time series. Rf1–Rf6 stands for right FOE's #1 to #6 (right panel) and Lf1–Lf6 stands for left FOE's #1 to #6 (left panel).

To uncover the hierarchical organization in the scalp and the mesial areas covered by the electrodes, we convert the correlation estimate in a measure which gives a more appropriate sense of “distance” among different regions. Following Gower (1966) we convert correlation, which is a dissimilarity measure $-1 < \delta_{ij} < 1$, to distance, which is a similarity measure, in the following way:

$$\rho_{ij} = \text{absolute value}(\delta_{ij}) \quad (2)$$

$$d(i,j) = \sqrt{\rho_{ii} + \rho_{jj} - 2\rho_{ij}} = \sqrt{2(1 - \rho_{ij})} \quad (3)$$

Distances are represented on a distance matrix for each pair of electrodes i,j . The classical agglomerative single-linkage algorithm was used with the objective to construct a hierarchical organization of interactions, or dendrogram.

By identifying clusters of synchronous activity in the mesial region it is possible therefore to identify also those areas whose activities are not synchronized, that is, those electrodes which cannot be assigned to a particular cluster of synchronous activity. We shall call those not synchronized electrodes as *desynchronized electrodes* (DE).

In addition to the linear correlation coefficient (1), we have also implemented the concept of phase synchronization, introduced firstly by Rosenblum et al. (1996), which has been increasingly used in the last years. Phase synchronization is a more general measure of synchrony between two time series, independent of the signals amplitude (Rosenblum et al., 2001).

For a continuous signal $x_i(t)$ the associated analytical or complex signal is defined as:

$$z_i(t) = x_i(t) + i\tilde{x}_i(t) = A_i(t)e^{i\phi_i(t)}$$

where $\tilde{x}_i(t)$ is the Hilbert transform of $x_i(t)$

$$\tilde{x}_i(t) = \frac{1}{\pi} p.v. \int_{-\infty}^{\infty} \frac{x(t')}{t-t'} dt' \quad (4)$$

where *p.v.* stands for (Cauchy) Principal Value. The instantaneous phase is thus,

$$\phi_i(t) = \arctan \frac{\tilde{x}_i(t)}{x_i(t)} \quad (5)$$

And the phase difference between the two signals can be calculated as:

$$\phi_i(t) - \phi_j(t) = \arctan \frac{\tilde{x}_i(t)x_j(t) - x_i(t)\tilde{x}_j(t)}{\tilde{x}_i(t)x_j(t) + x_i(t)\tilde{x}_j(t)} \quad (6)$$

In order to implement numerically the above definition over two time series $x_i(k)$ and $x_j(k)$, the mean phase coherence (R_{ij}) was introduced (Mormann et al., 2000):

$$R_{ij} = \left| \frac{1}{N_{win}} \sum_{k=1}^{N_{win}} e^{i\Delta\alpha_{ij}(k)} \right| \quad (7)$$

calculated in the time window N_{win} , where $\Delta\alpha_{ij}(k) = \phi_i(k) - \phi_j(k)$ is the instantaneous phase difference at the discretized time k . It is clear from (7) that R_{ij} follows the same relation that (2), that is $0 \leq R_{ij} \leq 1$. Calculations done with R_{ij} between two channels i and j will be called generically PS.

Again, as was done with correlation, a distance is introduced by using (3) but replacing $\rho_{ij} = R_{ij}$, instead of (2). In this way, a new hierarchical organization can be constructed based in PS.

2.3. Lateralization

The asymmetrical desynchronization pattern can be readily quantified for clinical use by using a lateralization index. For a given quantity M measured at the left and right temporal sides, M_L

and M_R respectively, lateralization has been described using the following index:

$$LI = (M_L - M_R)/(M_L + M_R) \quad (8)$$

If $M_L \gg M_R$, LI results in a value close to 1, implying a complete left-lateralization, and inversely, a LI close to -1 indicates a complete right lateralization.

We can take advantage of (8) by defining as a measurable quantity the number of DE per minute (rate) in each temporal side. In other words, we will quantify the number of those electrodes that do not belongs to a synchronization cluster in a particular temporal window. In this way we will call DE_L the number of DE per minute in the left mesial side and correspondingly, DE_R will be the number of DE per minute in the right side. We define analogously the lateralization index for the rate of DE as:

$$LI = (DE_L - DE_R)/(DE_L + DE_R) \quad (9)$$

2.4. Statistical analysis

When comparing two distributions from a particular measure, we will perform a two-tailed Wilcoxon signed rank test, testing the null hypotheses that there exists no difference between the calculated measures at both temporal lobes.

3. Results

3.1. Clusterization of brain activity

Fig. 2A shows a typical distance matrix for the whole set of electrodes in a single temporal window. It is readily apparent the division in two blocks, one for the scalp electrodes and the other for FOE. Darker regions correspond to tighter interactions, which are located mainly in the mesial area. This is expected since inter-electrode distance in scalp (4–5 cm) is greater than the inter-electrode distance in the FOE (1 cm). However, as can be observed in this Fig. 2A, there is a subtle differences between the left and right electrodes. In this example, left FOE (labelled as Lf1–Lf6) are more tightly connected among them (darker area in the matrix) than the right FOE. Fig. 2B shows the dendrogram corresponding to the distance matrix, built it by using the single-linkage method. The two big blocks observed in Fig. 2A are now clearly understood in Fig. 2B. One of them corresponds to the scalp electrodes, the big cluster at the half lower part of Fig. 2B, and the other one to the FOE (the half upper cluster). The branch corresponding to scalp electrodes is also subdivided in three sub-branches. Note that stronger interactions are represented as “deeper” positions in the dendrogram, as it is the case of electrodes C3–T3. One can consider the structure of the scalp electrodes as three “sub-clusters”, one composed of electrodes F7–F3–T3–C3–T5–O1 (peripheral left hemisphere), another by electrodes F8–T4–C4–T6–O2 (peripheral right hemisphere) and another one by electrodes Fp2–F4–P4–Fp1–P3 (parasagittal midline). However, a big difference exists between them due to their locations within the dendrogram. By comparing, for example the cluster F8–T4–C4–T6–O2 against Fp2–F4–P4–Fp1–P3 one can readily note that, interactions among electrodes inside the first cluster are much more tight connected than the electrodes inside the second one. In this sense, the cluster F8–T4–C4–T6–O2 is more robust than the cluster Fp2–F4–P4–Fp1–P3.

In the mesial area we found something similar. There exist a big cluster comprised by electrodes Lf1–Lf2–Lf3–Lf4–Lf5–Lf6–Rf1–Rf2–Rf3 and three electrodes which seems to be isolated, or not contained in any other cluster, as are electrodes Rf4, Rf5 and Rf6.

In Fig. 3 we represent the electrode locations, for the scalp in the traditional 10–20 position and for the FOE locations. Because FOE

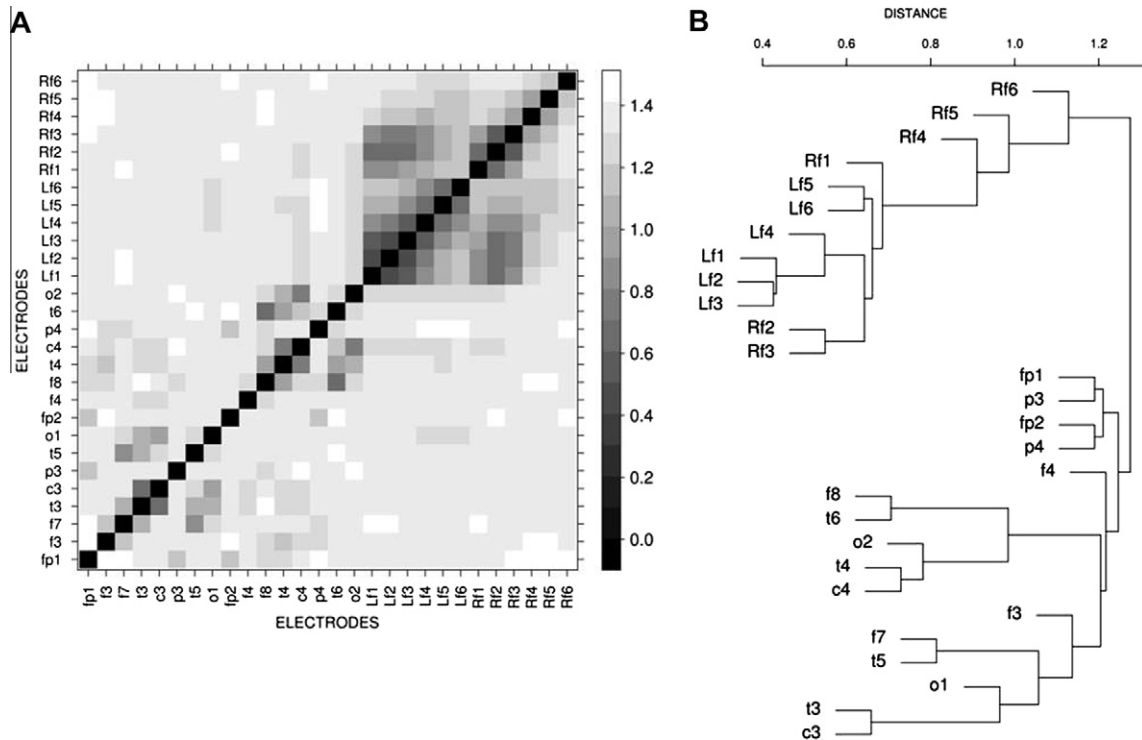


Fig. 2. (A) Distance matrix for a particular temporal window. Rf1–Rf6 stands for right FOE's #1 to #6. Rf1 is the most rostral electrode. Lf1–Lf6 stands for left FOE's #1 to #6. Lf1 is the most rostral electrode. The other labels are according with the standard 10–20 nomenclature. (B) Dendrogram extracted by using the agglomerative single-linkage procedure from the distance matrix (see text for explanations).

locations are actually in the inner part of the temporal lobe, we choose to represent their positions in between F3–C3–P3 and F7–T3–T5. This is a suitable approximation for a two-dimensional visualization although it is certainly not correct. In Fig. 3 electrode locations belonging to particular clusters are colored accordingly in a gray-scale. As noted previously in the dendrogram, most of

the right scalp electrodes belongs to a synchronization cluster, namely the F8–T4–C4–T6–O2 cluster. This implies that those electrodes are synchronized among them. This group is identified as a cluster because its low position in the dendrogram, which means that electrode positions within the cluster are highly synchronized. The other two groups of scalp's electrodes are not elected as clusters because interactions among their members are rather low. In this way, from all of the scalp electrodes, only one cluster is identified, the F8–T4–C4–T6–O2 cluster. This cluster is identified in Fig. 3 by filling their members with a light gray.

In the mesial area, as discussed previously, it is possible to identify only one cluster, comprised of electrodes Lf1–Lf2–Lf3–Lf4–Lf5–Lf6–Rf1–Rf2–Rf3. The other three right electrodes cannot be assigned to any other cluster. In this way, mesial electrodes belonging to this cluster are tinted as dark gray in Fig. 3. The remaining three electrodes are *declusterized* and therefore represented as empty white circles.

3.2. Dynamics of synchronization in mesial regions

In order to dig farther into this fact, we have carried out an automatic procedure to identify clusters of synchronous activity in every temporal window. Temporal windows of 10.24 s (2048 data points sampled at 200 Hz) have been used in records of typically 60 min, yielding approximately 360 temporal windows. To detect automatically synchronization clusters, we have used a recently published algorithm (Langfelder et al., 2008) aimed to identify clusters in hierarchical structures, like the one depicted in Fig. 2. Given a minimum number of electrodes the clusters must have, n , the algorithm automatically extract and identify all the clusters contained in the dendrogram with at least n members. Those remaining electrodes not belonging to any clusters continues unassigned and will be labeled as DE.

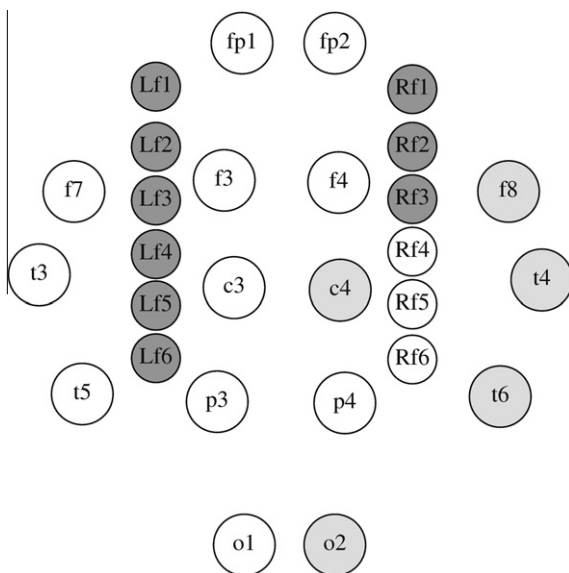


Fig. 3. Clusters of synchronous activity in scalp and FOE's. Different gray's levels are used to indicate synchronous clusters. Empty (white) electrodes cannot be assigned to a particular cluster, i.e. they are declusterized. In this window there exist three clusters. The whole right FOE's Rf1 to Rf6, four left FOE's, Lf3 to Lf6 and a scalp cluster C3–T3–T5–O2–C4–T4.

3.3. Clinical significance of declusterization

We have calculated the number of DE in the mesial area in each temporal lobe. In doing so, we count in each temporal window the number of mesial electrodes that cannot be assigned to any cluster, i.e., the number of DE. For instance in Fig. 3 there are three DE in the right FOE and zero DE in the left FOE. These numbers, 3 and 0, corresponds to the particular temporal window analyzed, and they may change in the previous and/or subsequent temporal windows. We have calculated these numbers along the whole record for each patient.

In the Fig. 4 we show a typical outcome from a patient's record (patient #3, $n = 3$, awake; see below) of 55 min, showing a larger synchronization in the left mesial area (lower panel) than the synchronization in the right mesial area (upper panel). The low synchronization activity is expressed by the great amount of DE, which sometimes is as high as 5 (for example around minute 7), that is, five out of the six electrodes cannot be assigned to a synchronization cluster.

We carried out the same former calculations in a sample of 17 patients suffering from TLE. When it was possible, that is, when EEG-FOE records were free of artifacts and of suitable quality for numerical analysis, the analysis was done in two different situations, with the patient in awake and sleep states.

Table 2 shows the main results of our findings. To generate as much as valuable information as possible, we have included also three different numbers for each state. These three columns, numbered as 2, 3, and 4 for each awake and sleep corresponds to the minimum number of electrodes a cluster must have to “deserve” to be a cluster, that is, n . That is, when a cluster has at least 3 members (electrodes), a cluster of only two electrodes is not considered as a cluster. This information is important at the time to explore the cluster organization, and also to assess the invariance of the synchronization activity, regardless of the cluster definition.

By counting the number of DE in each side, and dividing this number by the total time, we can use (9) in order to calculate

the LI , and therefore quantify the (im)balance in synchronization. In Table 2 we have shaded those LI in between -0.1 and 0.1 (light grey), because its low lateralization power. We have also shaded (dark grey) those LI which are opposed to the overall diagnosis. There are three of these cases, patients #14, #15 and #17.

It is clear the strong relation existing between the asymmetrical distribution of DE and the overall lateralization diagnosis. For every patient, except patient #17, both awake and sleep LI has the same sign, although there exists quantitative differences in several cases (compare for instance case #1 against case #4). In all but two cases (patients #12 and #17) LI is consistent with the physician diagnosis, which is based in pre-surgical studies, but primarily in the v-EEG and IED analysis. One of these cases, patient #12 is an Engel III with multifocality as diagnosed by v-EEG and SPECT studies.

Patient #14 and also patient #17 fail in identifying the correct epileptic side (as indicated by diagnosis) in the case of a cluster definition with a minimum number of members equal to four ($n = 4$). This is due to the intrinsic structure of the dendrogram and the hierarchies of electrodes. The whole set of six electrodes in the contra-lateral side is divided in two groups of three electrodes, namely Rf1-Rf2-Rf3 and Rf4-Rf5-Rf6, in the case of patient #14, due to the strong interactions among them and the automatic algorithm of cluster identification, which is “tuned” to recognize clusters comprised of at least four electrodes. Thus, it fails to identify both groups as a unique cluster, and therefore leaves the whole set of contra-lateral electrodes as DEs. When the minimum number of electrodes needed to define a cluster is lower than four, however, the algorithm correctly lateralizes the epileptic side, mainly when the minimum number is two.

Case #15 is a different one, because there are very low interactions among the electrodes both in the ipsi and in the contra-lateral side, yielding therefore a similar number of DE in both sides.

Note in Table 2 that in all cases but two, namely patient #12 and patient #15, physician lateralization match cluster analysis lateralization. Patient #12 however is not only an Engel III surgery

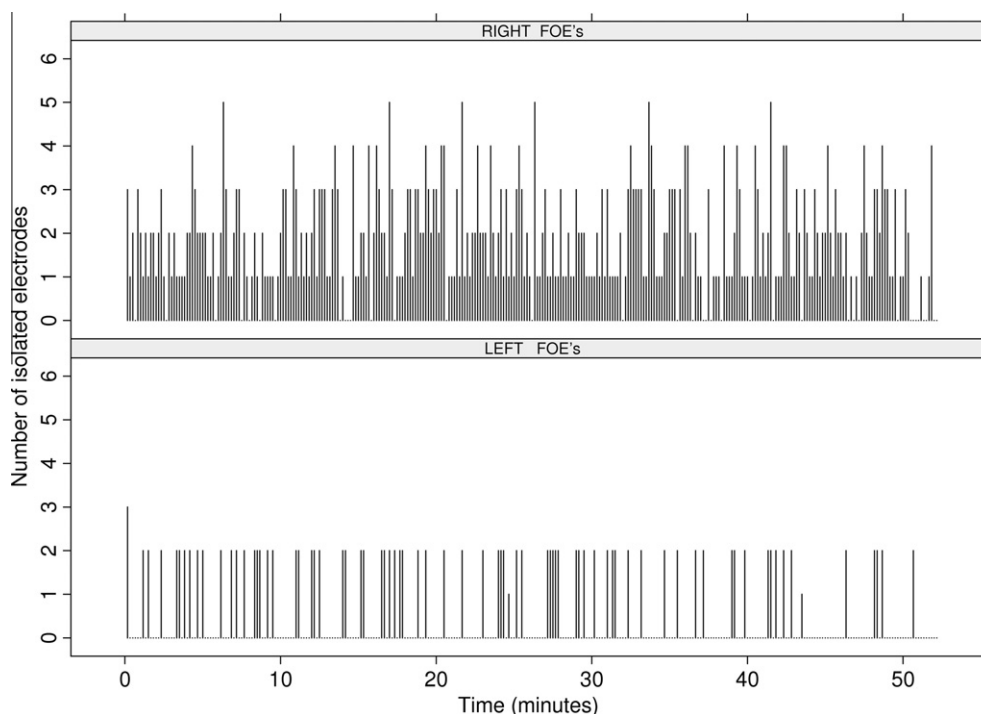


Fig. 4. Number of isolated electrodes as a function of time for a typical record (patient #3, $n = 3$, awake). Both right and left FOE's not assigned to any cluster, DE, in a record of 55 min.

Table 2
Cluster and synchronization results.

Patient	Cluster analysis							Local sync. (%)	IED analysis			
	$LI = (L - R)/(L + R)$								IED/min	LI	Side	
	Awake			Sleep								
2	3	4	2	3	4	Side	R	L				
1	0.99	0.99	1	0.99	0.97	0.97	L	0.25	0.00	2.01	1.00	L
2	-0.87	-0.75	-0.9	-1	-0.3	-0.8	R	2.2	5.78	0.12	-0.96	R
3	-0.98	-0.57	-0.97	-1	-0.92	-1	R	4.68	2.14	0.05	-0.96	R
4	-0.05	-0.26	-0.05	-1	-0.9	-0.12	R	15.04	3.88	1.59	-0.42	R
5	-0.59	-0.5	-0.19	-0.89	-0.71	-0.	R	3.01	2.31	0.03	-0.98	R
6	0.41	0.8	0.68	NA	NA	NA	L	0	2.34	2.36	0.00	
7	0.91	0.6	0.69	1	0.35	0.91	L	2.91	0.59	3.93	0.74	L
8	1	0.76	0.89	NA	NA	NA	L	0.5	0.38	2.85	0.76	L
9	0.76	0.5	0.25	NA	NA	NA	L	30	2.06	6.87	0.54	L
10	0.19	0.58	0.39	NA	NA	NA	L	19.1	0.41	2.43	0.71	L
11	0.69	0.64	0.65	NA	NA	NA	L	60.51	1.83	5.43	0.50	L
12	-0.02	0.02	-0.01	0.18	0.29	0.28	L	22.73	3.11	0.64	-0.66	R
13	0.21	0.05	0.38	0.44	0.42	0.59	L	22.35	2.34	3.93	0.25	L
14	0.32	0.43	-0.54	0.88	0.57	-0.03	L	24.92	0.35	1.33	0.58	L
15	0.03	-0.14	-0.08	0.3	-0.23	0		26.61 ^a	4.26	1.52	-0.47	R
16	0.85	0.72	0.73	0.99	0.93	0.91	L	13.64	1.06	4.87	0.64	L
17	0.94	0.07	0.18	1	-0.01	-0.17	L	44.14	0.65	2.19	0.54	L

Local sync: Percentage of time where maximum of synchronization is located in the focal side.

^a Local sync referenced to the left side.

outcome, but moreover, interictal video-EEG and SPECT analyses gives clues of at least a multifocal origin of seizures, and therefore must be taking with care for further analysis. In fact surgery decision was based solely for palliative purposes. On the other side, patient #15 seems to be unexplained by this solely analysis.

3.4. Declusterization is based upon lower synchronization activity

The results seem to favour the conclusion that the epileptic side display lowers levels of synchronous activity than the contra-lateral side, because the higher number of DE in the ipsi-lateral side. Greater number of DE, lower levels of synchronization activity. To corroborate this conclusion in an independent way of the clusterization algorithm, we have calculated the average (actually the median) “distance” in each mesial side (Schiff et al., 2005) coming from all the FOE in that side, by summing up distances between each mesial electrode with every other electrode in the same mesial side. The average distance is divided by two because the symmetric character of distance. Naming $Sync_L$ and $Sync_R$ to the average synchronization (Sync) at the left and right mesial sides respectively, we calculate the lateralization index LI using (8). From now on, we shall work only with the awake files in order to have a complete set of records (see Table 2).

In Fig. 5A we plot LI for both Sync and DE ($n = 2,3,4$). As expected, there exist a high correlation between both lateralization measures. For $n = 2$, that is, clusters of at least two electrodes, the correlation between LI of DE and Sync is 0.9116 ($p < 0.001$). For $n = 3$ the correlation is 0.903 ($p < 0.001$), and in the case of $n = 4$, the correlation coefficient is 0.84 ($p < 0.001$). In this last case, there exist one case, namely patient #14 where both measures yield opposite and relative high values, that is why the correlation coefficient is lower than in the other two cases. In overall, it seems that DE performs much better than synchronization as a lateralization method, since it takes higher values. In the next sections we shall calculate one more lateralization measure and statistically compare synchronization and DE.

3.5. Epileptic rigidity revisited

In contrast to the case of IHDE analysis, there exist little analysis of FOE activity outside the framework of IED realm. Notable excep-

tions are Wang and Wieser, 1994 and Weber et al., 1998. In both cases, although with very different approaches, they show the existence of an imbalance regarding complexity or variability between both mesial areas in TLE. In Wang and Wieser, 1994, a significant difference is shown between the variability at both sides, quantified by alterations in the total power spectrum of the FOE signals. Weber et al. found equivalent results, showing that the epileptic side shows lowers levels of complexity, as quantified by the correlation dimension. They were able to correctly lateralize the epileptic area in 16 out of 19 patients.

In order to complete our analysis, we shall also analyse complexity in our patient's sample, but from a somewhat equivalent point of view. Instead of using spectral properties or correlation integral (and embeddings), we have calculated permutation entropy (PE) (Bandt and Pompe, 2002), which is a robust measure of complexity, where greater complexity would imply less rigidity. We have calculated PE, of order 4, in each FOE channel, in each temporal window and lastly we summed up PE estimates for all the electrodes at both, the epileptic and the contra-lateral sides. This therefore yields two time series with PE for each side. Again, as in the case of synchronization, we use the median of both time series to estimate the rigidity at both mesial sides. Results are presented in the next subsection.

3.6. Significance of lateralization measures

We will evaluate the statistical significance of these three measures, Sync, DE and PE, as lateralization techniques. Wilcoxon signed rank test for each patient was calculated for the three measures; Sync, DE ($n = 3$) and complexity (PE), testing the null hypotheses that there exist no difference between a particular measure at both temporal lobes, that is: $Sync_L = Sync_R$, $DE(3)_L = DE(3)_R$ and $PE_L = PE_R$.

In Fig. 5B we represent the significance in rejecting the null hypothesis of equal measure (for the three quantities) in every patient. In the case of synchronization (blue), there exist significant differences ($p < 0.001$) between synchronization between the ipsi and contra-lateral side, which implies that the lateralization index in Fig. 5A is robust in all of the patients in the sample. In the case of DE ($n = 3$) (red) however, there are four cases, namely patients #13, #4, #12 and #15 with no evidence against the null hypothesis. The

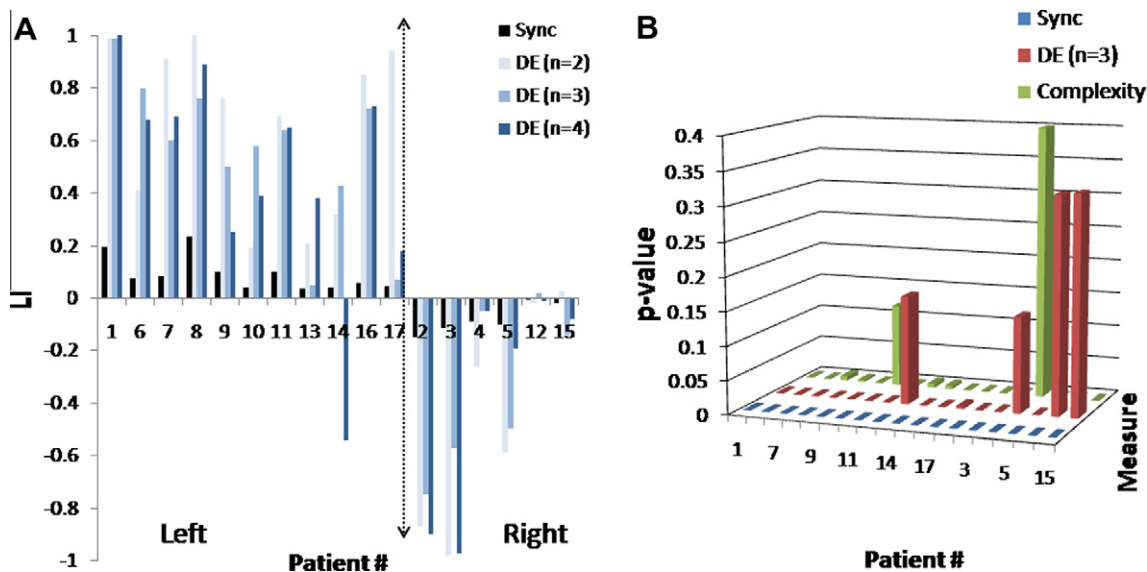


Fig. 5. (A) *LI* for synchronous activity (Sync), in black bars and declusterized electrodes (DE) activity in bluish bars. Patients are ordered according with the physician diagnosis regarding lateralization. Dotted line arrow separate left temporal epileptic patients (patients 1,6,7,8,9,10,11,12,14,16 and 17) from right temporal epileptic patients (patients 2,3,4,5,12 and 15). In the case of DE, $n = 2,3,4$ stands for the minimum number of electrodes a cluster must have (see text). (B) Significance for the lateralization measures, synchronization (Sync), declusterized electrodes (DE) and complexity.

same happens for the complexity measure (green), in two cases, patient #10 and patient #4 ($p > 0.05$).

Overall, the statistical test shows that there exist a clear difference in synchronization levels between the ipsi and the contra-lateral sides and in this way, the *LI* displayed in Fig. 5A is a trustable indicator of the epileptic side.

3.7. Maximal synchronization site

We also sought for the highest synchronization activity site (local maxima). To do that we have located the minimum distance between two different electrodes in the same side, in the distance matrix in each temporal window, and then we lateralize this value, right or left accordingly in which side was found. We then calculate the percentage of time (number of temporal windows) the minimum is at the same side of higher synchronization, as calculated before. We present these results in Table 2, “Local Sync. (%)” column. As expected, in most of the cases (15 out of 17) the maximal synchronization activity between two electrodes is located at the contra-lateral side, most of the time (more than 50% of the total number of windows), where the average synchronization is also high.

3.8. Synchronization and IED

IED are known to be present in the electrophysiological records of TLE patients and, from its very definition they can affect synchronization of background activity. As it is usual, an IED is defined (Pastor et al., 2010) when spikes appears simultaneously in at least three consecutive channels in the bipolar montage of FOC records. We have included in Table 2 the IED information for each patient, which it is in accordance with typical values reported in the literature (Clemens et al., 2003; Pastor et al., 2010). There is a prevalence of IED in the ipsi-lateral side, which in turn could reinforce synchronization levels in this temporal side. Therefore, a potential influence of IED in the correlation estimate (1) must be addressed. In order to explore this fact, we have made the following theoretical calculation. A single IED structure typically last at most 400 ms (Zumsteg et al., 2006). In our patient sample, the maximum num-

ber of IED is 81, counted in a window of ten minutes (patient #9), which in turn results in a total “IED time” of $81 \times 0.4 = 32.4$ s. Therefore, in 10 min, 32.4 s represents $32.4 / (10 \times 60) = 0.054$ or 5.4% of the total time. Thus, IED are present at most 5.4% of the time in a typical record. Average values for the epileptic side (see Table 2) gives 3.51 IED/min, which in turn gives 2.3% of IED time. In order to address the question whether or not IED time affects the correlation calculation, we have implemented the following procedure. We have generated two Gaussian stochastic processes with a given value of correlation and we have replaced part of the records by a simulated IED. The simulated IED, represented by a sine wave cycle, is inserted at the same time in both time series. In this way we can study the influence of IED time, on the correlation estimate by increasing the proportion of the IED time in the records, ranging from 0% (no IED) to 100% (a whole IED). Lastly we have plotted the ratio between $\rho(\text{stoch}, \text{stoch})$, that is, the correlation between both purely stochastic process, to $\rho(\text{stoch} + \text{IED}, \text{stoch} + \text{IED})$, the correlation between the processes with the inserted simulated IED, $\rho(\text{stoch}, \text{stoch}) / \rho(\text{stoch} + \text{IED}, \text{stoch} + \text{IED})$. This is showed in Fig. 6. As can be seen, for small levels of correlation between both signals the influence of IED time is much higher (left part of the figure) than the case of high levels of correlation (right part), and also for high proportion of IED time (upper left part). In our case, the maximum IED time in the data is 5.4%, as we mentioned above. What we need to know in order to use the theoretical calculation and Fig. 6 is the correlation between pairs of electrode records. The average correlation between every pair of different FOC channels, for every patient, gives an average correlation of 0.51 ± 0.12 . Thus, for an average Pearson correlation of 0.51 (x -axis) and a maximum percentage of IED time (y -axis) of 5.4, we can conclude from Fig. 6 that we are in a very safe location, where IED time, at those levels of correlation, hardly affects Pearson estimate. We have also plotted in Fig. 6 the area approximately covered by the sample data used.

Note finally that if IED could affects correlations values, it would be by increasing synchronization in the ipsi-lateral side, because the greater number of them in that side. As we have demonstrated above, synchronization is lower in the ipsi-lateral side, so it is highly improbable the IED can be the reason of this fact.

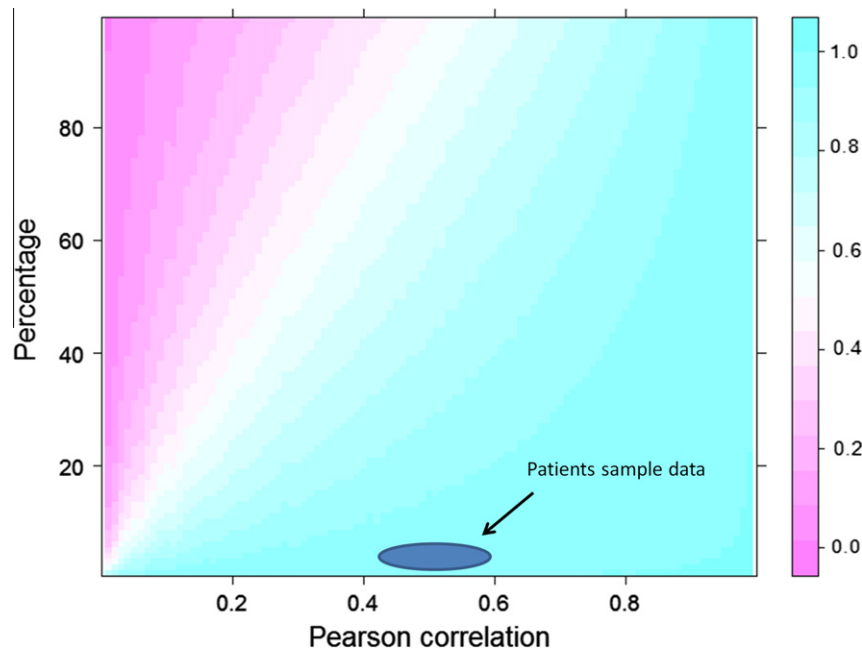


Fig. 6. Different patterns of time shifts between FOE records. (A) No time shift between any of the FOE records. This pattern appears in 7 of the 17 patients. (B) Unique record (patient #2) with a lag pattern compatible with a signal propagation. (C) Other kind of time shifts between FOE records, incompatibles with a signal propagation (9 out of 17 patients). (D) Synchronization values for every patient using cross-correlation (CC) and Phase Synchronization (PS). Vertical solid black line separates left from right TLE. Horizontal dashed line separates Phase synchronization from cross correlation.

3.9. Desynchronization and propagation

Lastly we have tested for a possible signal propagation throughout the mesial structure. This is especially important since there has been previous reports that IED propagates in TLE patients (Zumsteg et al., 2006 and references therein). Although we have demonstrated in the previous section that IED does not affect the analysis already carried out, we have investigated nonetheless whether exists any kind of signal propagation through the mesial areas. In order to do that, we have calculated the lags, in terms of sampling time, where the cross-correlation reaches its maximum, for every pair of EFO channels. In Fig. 7 we display three typical results. In Fig. 7A we can observe that no time shift between pairs of EFOs exists. This kind of pattern is incompatible with the existence of signal propagation at the time resolution used. In the analyzed patients sample, 7 out of 17 patients shows this kind of pattern. In Fig. 7B however, Rf4 and also Rf6 shows a lags pattern consistent with a signal propagation, but this is the unique case (patient #2). The remaining 9 patients shows a lags distribution as showed in Fig. 7C. In this case just one or two lags are different from zero, which evidently is incompatible with a signal propagation across the mesial structure.

As a further test of the reliability of our results, we have repeated the same whole procedure in calculating DE, but using phase synchronization (see Methods), instead of the correlation coefficient. In Fig. 7D we compare results of both measures, Pearson cross-correlation (CC) and phase synchronization (PS). It is readily apparent that, at least qualitatively, both synchronization measures behaves in the same fashion, with minor differences between them. Note that in the half lower part of Fig. 7C, below the dashed line, corresponding to CC, the representation is the same as the Fig. 5A for the three different number of DE.

4. Discussion

Our results show a synchronization imbalance between ipsi and contra-lateral mesial areas in TLE patients, during the inter-ictal

state. Synchronization patterns have been quantified here by the property of being part of a synchronization cluster or not. Those mesial areas belonging to any cluster have therefore its activity well synchronized with other areas within the cluster. On the opposite, those regions which are not member of any cluster are therefore desynchronized from the rest, i.e., they are declusterized regions. In TLE patients the areas covered by the FOE in the epileptic side behaves highly declusterized. In the contra-lateral side, conversely, mesial sites have a tendency to behave synchronized among them within one or several clusters. This fact has been quantified here by the *LI* and its comparison with pre-surgical diagnosis and/or surgery-outcome shows its power as a trustable lateralizer.

As we have also shown, declusterization is directly related with average desynchronization in the whole side. The higher levels of declusterization displayed in the epileptic side produce low levels of synchronization. We have also calculated the degree of complexity (or lack of rigidity) in both sides, showing that the epileptic side displays lower levels of complexity than the contra-lateral one, in accordance with previous works (Wang and Wieser, 1994; Weber et al., 1998).

One important point to be discussed is the apparent disagreement with previous works related with synchronization analysis in the mesial area (Mormann et al., 2000; Andrzejak et al., 2006; Bettus et al., 2008; Bartolomei et al., 2008) where it is reported higher levels of interictal synchronization in the epileptic side as compared against the contra-lateral side. However, those works are based on analysis carried out with IHDE records, very different with the one analyzed here, coming from FOE. It is known that FOE does record activity in extrahippocampal areas, as the entorhinal cortex and the parahippocampal gyrus. In contrast, IHDE are located, in addition to the entorhinal cortex, in other structures as amygdala and hippocampus for instance. Besides that, in some of these studies, band limited analysis, linear and nonlinear, has been employed, in contrast with the broad band analysis used in our work. For instance, it has been recently reported (Mormann et al., 2008) that there exist different synchronization patterns in

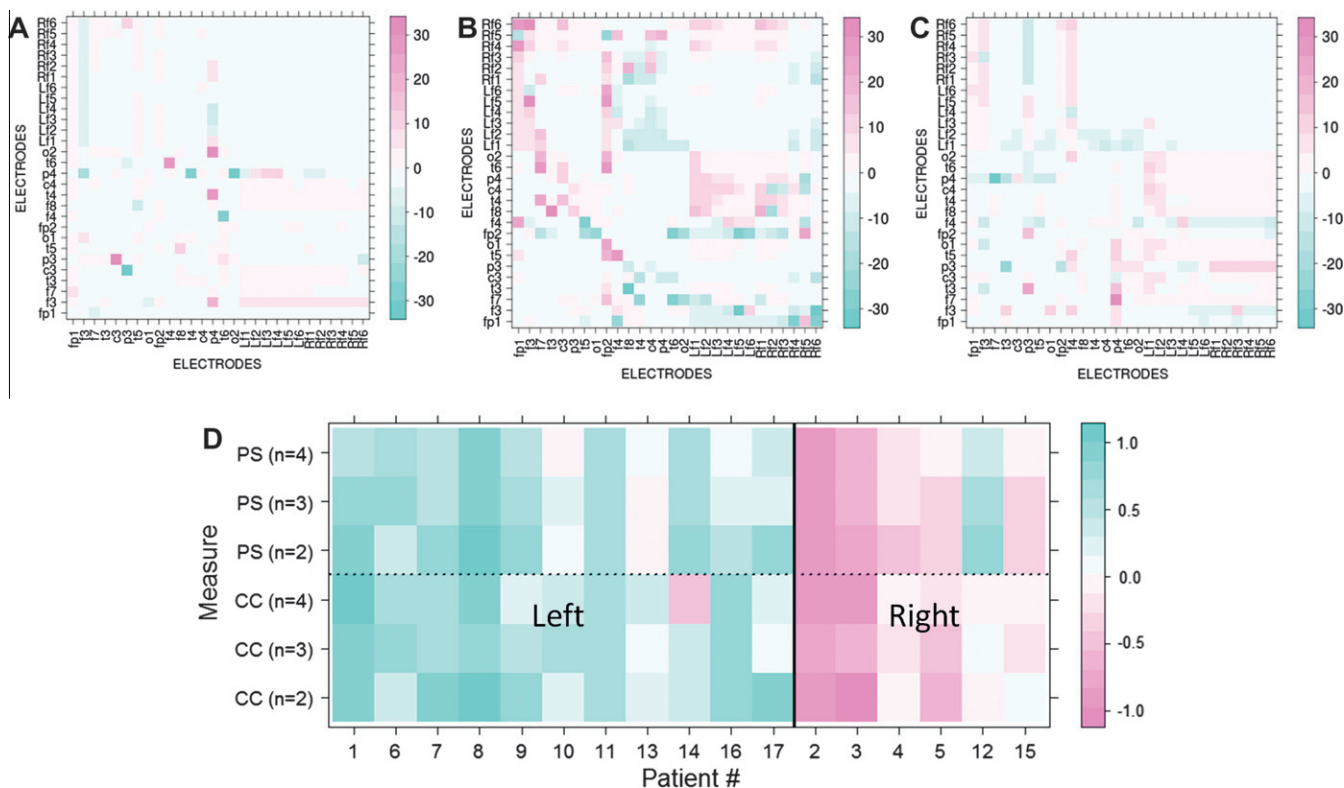


Fig. 7. Influence of IED time in correlation values: Ratio of $\rho(\text{stoch}, \text{stoch})$ to $\rho(\text{stoch} + \text{IED}, \text{stoch} + \text{IED})$, as a function of correlation value, of two Gaussian stochastic process (x-axis) and the percentage of IED-time (y-axis). Blue ellipse represents correlation and average IED time in data from the sample records. See text for full explanation.

entorhinal cortex and in intrahippocampal areas, but restricted to the delta and theta bands.

Our results are important from two points of view. First, the lateralization power displayed by the three measures, synchronization, DE and complexity, outside the framework of the spike analysis technique, which is nevertheless the most common usage in FOE analysis in TLE patients, gives new perspectives and potential values to FOE technique in the study of epilepsy, mainly bearing in mind its less invasiveness character than for example IHDE (Pastor et al., 2008).

Secondly, and comparing with traditional EEG + FOE studies, the methodology describes here not only would reduce the analysis time drastically, but moreover in combination with the use of drugs able to activate the epileptogenic zone (Pastor et al., 2010), in one or two hour of interictal activity it would be possible to extract reliable conclusions regarding the lateralization. This fact is particularly relevant from a diagnostic point of view.

Epilepsy is a very complex structural and dynamical disease, where the interplay among, known and unknown factors result in the clinical seizures. Identification, prediction and control of some of these factors are fundamental in the road to the epileptic seizures' control or elimination. The results presented here could open new insight in devising such strategies, in the case that mesial synchronization plays a central role in the seizure appearance. In this sense, one could speculate that the synchronization imbalance between both mesial sides may be "balanced" by electrical stimulation by using a device chronically implanted (Velasco et al., 2007), similar to the electrodes used for Deep Brain Stimulation. However, too many questions must be answered before such a technique could be reliably implemented.

Acknowledgments

This work has been funded by grants from the Fundación Mutua Madrileña (GJO, JP) and from the Plan Nacional de Investigación Científica, Desarrollo e Innovación Tecnológica (I + D + I), Instituto de Salud Carlos III, PS09/02116 (JP e I.H.P.) and PI10/00160 (GJO); Proyectos de investigación de la Universidad San Pablo-CEU, PPC9/09 (JP, GJO, RGS). IHP is predoctoral investigator from the Biomedical Foundation of Investigation, Hospital Universitario La Princesa, Universidad Autónoma de Madrid. GJO acknowledge financial support from the Instituto de Salud Carlos III through a Miguel Servet research contract. The authors wish to thank the reviewers for their constructive comments.

References

- Andrzejak R, Mormann F, Widman G, Kreuz T, Elger C, Lehnertz K. Improved spatial characterization of the epileptic brain by focusing on nonlinearity. *Epilepsy Res* 2006;69(1):30–44.
- Bandt C, Pompe B. Permutation entropy: a natural complexity measure for time series. *Phys Rev Lett* 2002;88:174102.
- Bartolomei F, Chauvel P, Wendling F. Epileptogenicity of brain structures in human temporal lobe epilepsy: a quantified study from intracerebral EEG. *Brain* 2008;131:1818–30.
- Bettus G, Wendling F, Guye M, Valton L, Regis J, Chauvel P, Bartolomei F. Enhanced EEG functional connectivity in mesial temporal lobe epilepsy. *Epilepsy Res* 2008;81:58–68.
- Clemens Z, Janszky J, Szucs A, Békésy M, Clemens B, Halász P. Interictal epileptic spiking during sleep and wakefulness in mesial temporal lobe epilepsy: a comparative study of scalp and foramen ovale electrodes. *Epilepsia* 2003;44(2):186–92.
- Dichter MA, Ayala GF. Cellular mechanism of epilepsy: a status report. *Science* 1987;237:157–64.
- Engel J. *Seizures and Epilepsy*. Philadelphia, PA: FA Davis; 1989.
- Engel J, Van Ness PC, Rasmussen TB, Ojemann LM. Outcome with respect to epileptic seizures. In: Engel Jr J, editor. *Surgical treatment of the epilepsies*. New York: Raven Press; 1993. p. 609.

- Fein G, Raz J, Brown FF, Merrin EL. Common reference coherence data are confounded by power and phase effects. *Electroencephalography Clin Neurophysiol* 1988;69:581–4.
- Gower JC. Some distance properties of latent root and vector methods used in multivariate analysis. *Biometrika* 1966;53:325–8.
- Guevara R, Velazquez JL, Nenadovic V, Wennberg R, Senjanovic G, et al. Phase synchronization measurements using electroencephalographic recordings: what can we really say about neuronal synchrony? *Neuroinformatics* 2005;301–14.
- Gutkin BS, Lang CR, Colby CL, Chow CC, Ermentrout GB. Turning on and off with excitation: the role of spike-timing asynchrony and synchrony in sustained neural activity. *J Comput Neurosci* 2001;11:121–34.
- Kandel ER, Schwartz JH, Jessell TM. *Principles of Neural Science*. 4th ed. New York: McGraw-Hill; 2000.
- Langfelder P, Zhang B, Horvath S. Defining clusters from a hierarchical cluster tree: the dynamic tree cut package for R. *Bioinformatics* 2008;24(5):719–20.
- Mormann F, Lehnertz K, David P, Elger CE. Mean phase coherence as a measure for phase synchronization and its application to the EEG of epilepsy patients. *Physica D* 2000;144:358–69.
- Mormann F, Kreuz T, Andrzejak RG, David P, Lehnertz K, Elger CE. Epileptic seizures are preceded by a decrease in synchronization. *Epilepsy Res* 2003;53(3):173–85.
- Mormann F, Osterhage H, Andrzejak RG, Weber B, Fernández G, Fell J, Elger CE, Lehnertz K. Independent delta/theta rhythms in the human hippocampus and entorhinal cortex. *Frontiers in human cortex* 2008;2(3):1–6.
- Netoff TI, Schiff SJ. Decreased neuronal synchronization during experimental seizures. *J Neurosci* 2002;22:7297–307.
- Ortega GJ, Menéndez de la Prida L, García de Sola R, Pastor J. Synchronization clusters of interictal activity in the lateral temporal cortex of epileptic patients: intraoperative electrocorticographic analysis. *Epilepsia* 2008;49(2):269–80.
- Pastor J, Hernando V, Domínguez-Gadea L, De Llano I, Meilán ML, Martínez-Chacón JL, Sola RG. Impact of experience on improving the surgical outcome in temporal lobe epilepsy. *Revista de Neurología* 2005;41(12):709–16.
- Pastor J, Menéndez de la Prida L, Hernando V, Sola RG. Voltage sources in mesial temporal lobe epilepsy recorded with foramen ovale electrodes. *Clin Neurophysiol* 2006;117(12):2604–14.
- Pastor J, Sola RG, Hernando-Requejo V, Navarrete EG, Pulido P. Morbidity associated with the use of foramen ovale electrodes. *Epilepsia* 2008;49(3):464–9.
- Pastor J, Wix R, Meilán ML, Martínez-Chacón JL, de Dos E, Domínguez-Gadea L, Herrera-Peco I, Sola RG. Etomidate accurately localizes the epileptic area in patients with temporal lobe epilepsy. *Epilepsia* 2010;51(4):602–9.
- Penfield W, Jasper H. *Hypersynchrony. Epilepsy and the functional anatomy of the human brain*. Boston: Little, Brown and Company; 1954. p. 193–4.
- Quián Quiroga R, Kraskov A, Kreuz T, Grassberger G. Performance of different synchronization measures in real data: a case study on electroencephalographic signals. *Physical Review E* 2002;65:041903.
- Rosenblum MG, Pikovsky AS, Kurths J. Phase synchronization of chaotic oscillators. *Phys Rev Lett* 1996;76:1804–7.
- Rosenblum MG, Pikovsky AS, Kurths J, Schaefer C, Tass P. Phase synchronization: from theory to data analysis. In: Moss F, Gielen S, editors. *Handbook of biological physics*. Amsterdam: Elsevier Science; 2001. p. 297.
- Schiff SJ, Sauer T, Kumar R, Weinstein SL. Neuronal spatiotemporal pattern discrimination: the dynamical evolution of seizures. *Neuroimage* 2005;28:1043–55.
- Schindler K, Leung H, Elger CE, Lehnertz K. Assessing seizure dynamics by analyzing the correlation structure of multichannel intracranial EEG. *Brain* 2007;130:65–77.
- Sola RG, Hernando V, Pastor J, Navarrete EG, Felipe de J, Alijarde MT, et al. Pharmacoresistant temporal-lobe epilepsy. Exploration with foramen ovale electrodes and surgical outcomes. *Revista de Neurología*. 2005;41(1):4–16.
- Traub RD, Wong RK. Cellular mechanism of neuronal synchronization in epilepsy. *Science* 1982;216:4547–745.
- Velasco AL, Velasco F, Velasco M, Trejo D, Castro G, Carrillo-Ruiz JD. Electrical stimulation of the hippocampal epileptic foci for seizure control: a double-blind, long-term follow-up study. *Epilepsia* 2007;48(10):1895–903.
- Wang J, Wieser HG. Regional “rigidity” of background EEG activity in the epileptogenic zone. *Epilepsia* 1994;35(3):495–504.
- Weber B, Lehnertz K, Elger CE, Wieser HG. Neuronal complexity loss in interictal EEG recorded with foramen ovale electrodes predicts side of primary epileptogenic area in temporal lobe epilepsy: a replication study. *Epilepsia* 1998;39(9):922–7.
- Wieser HG, Elger CE, Stodieck SR. The ‘foramen ovale electrode’: a new recording method for the preoperative evaluation of patients suffering from mesio-basal temporal lobe epilepsy. *Electroencephalography Clin Neurophysiol* 1985;61(4):314–22.
- Wieser GH, Schwarz U. Topography of foramen ovale electrodes by 3D image reconstruction. *Clin Neurophysiol* 2001;112:2053–6.
- Zumsteg GH, Friedman A, Wieser HG, Wennberg RA. Propagation of interictal discharges in temporal lobe epilepsy: correlation of spatiotemporal mapping with intracranial foramen ovale electrode recordings. *Clin Neurophysiol* 2006;117:2615–26.